Comparison between Boolean and piecewise affine differential models for genetic networks

Madalena Chaves, Laurent Tournier, Jean-Luc Gouzé

INSTITUT NATIONAL DE RECHERCHE EN INFORMATIQUE ET EN AUTOMATIQUE

Comparison between Boolean and piecewise affine differential models for genetic networks

Madalena Chaves — Laurent Tournier — Jean-Luc Gouzé

N° 7070

October 2009

ISSN 0249-6399 ISRN INRIA/RR--7070--FR+ENG

INSTITUT NATIONAL
DE RECHERCHE
EN INFORMATIQUE
ET EN AUTOMATIQUE

INRIA

centre de recherche
SOPHIA ANTIPOLIS - MÉDITERRANÉE

Comparison between Boolean and piecewise affine differential models for genetic networks

Madalena Chaves*, Laurent Tournier†, Jean-Luc Gouzé*

Thème : Observation, modélisation et commande pour le vivant
Équipe-Projet COMORE

Rapport de recherche n° 7070 — October 2009 — 23 pages

Abstract: Multi-level discrete models of genetic networks, or the more general piecewise affine differential models, provide qualitative information on the dynamics of the system, based on a small number of parameters (such as synthesis and degradation rates). Boolean models also provide qualitative information, but are based simply on the structure of interconnections. To explore the relationship between the two formalisms, a piecewise affine differential model and a Boolean model are compared, for the carbon starvation response network in *E. coli*. The asymptotic dynamics of both models are shown to be quite similar. This study suggests new tools for analysis and reduction of biological networks.

Key-words: Boolean models, piecewise affine models, genetic networks, model reduction

* INRIA, project-team COMORE, 2004 Route des Lucioles, BP 93, 06902 Sophia Antipolis, France, {mchaves,gouze}@sophia.inria.fr

† INRA, Unité de Mathématique, Informatique et Génôme (UR 1077) Domaine de Vilvert, 78350 Jouy-en-Josas, France, laurent.tournier@jouy.inra.fr

Centre de recherche INRIA Sophia Antipolis – Méditerranée
2004, route des Lucioles, BP 93, 06902 Sophia Antipolis Cedex
Téléphone : +33 4 92 38 77 77 — Télécopie : +33 4 92 38 77 65

Comparaison entre modèles booléens et différentiels linéaires par morceaux ; application aux réseaux géniques

Résumé : Les modèles discrets (multi-niveaux), et plus généralement les modèles différentiels linéaires par morceaux, donnent des informations qualitatives sur la dynamique d'un système, en utilisant très peu de paramètres (comme les taux de synthèse et de dégradation d'une espèce). Les modèles booléens donnent aussi des informations qualitatives en partant seulement de la structure des interconnections. Pour examiner les rapports entre ces deux types de formalismes, cette étude mène une comparaison entre un modèle différentiel linéaire par morceaux et un modèle booléen, pour un réseaux génique lié à la réponse au stress en carbone de la bactérie *E. coli*. Cette étude suggère de nouveaux outils pour l'analyse et la réduction des modèles de réseaux biologiques.

Mots-clés : Modèles booléens, modèles linéaires par morceaux, réseaux géniques, réduction de modèles

1 Introduction

Genetic regulatory networks have been analysed through various different formalisms, in particular continuous differential models [17], piecewise affine (PWA) models [10, 8, 4], multi-level discrete models [13, 11], and Boolean models [6, 5, 3, 14]. Each formalism has its advantages and drawbacks, and different models using different formalisms may provide complementary information on the system. To illustrate this point of view, we will analyse the PWA model of the carbon starvation response in *E.coli* developed in [10], which was studied mathematically in [8]. An algorithmic method, consisting of two mains steps, will be proposed to construct a Boolean model from a piecewise affine model: first, the PWA system gives rise to a multi-level discrete system, where each variable takes values in a finite set; then the discrete model can be translated into a Boolean model, by appropriately extending the state space (see, for instance, [16]). (See Section 2 and Appendix 1).

The Boolean model has two attractors that correctly represent the asymptotic behaviour of the piecewise linear system, under two different input conditions. Following the method developed in [14], it is possible to identify a family of "operational interactions" for each attractor: a subset of the original network of interactions that actively contribute to characterize the dynamics within that attractor. This family of operational interactions, together with the components involved, constitutes a smaller (Boolean) subsystem of the original system, which can be used to construct a reduced model of the system of differential equations. The asymptotic dynamics of the PWA and Boolean model are compared and shown to agree in most qualitative aspects (Section 4). In particular, we illustrate the correspondance between a sliding mode in the PWA model [8] (which may induce chattering or Zeno behaviour [18] in one of the variables), and period 2 oscillations in the Boolean model (see Section 5). These results suggest future applications of Boolean network analysis to model reduction techniques.

2 Piecewise affine, discrete and Boolean models for genetic networks

To compare the results of discrete and Boolean modelling frameworks, we first briefly describe the different formalisms, and discuss some methods to transform a model from one formalism to the other without changing the dynamical behaviour. As an example, the model developed in [10] and studied in [8] will later be analysed. Throughout this section, for a system with $n > 0$ variables, let x_i ($i = 1, \ldots, n$) denote the continuous variables, V_i the corresponding discrete variables, each with a discrete set of values $V_i \in \{0, 1, \ldots, d_i\}$ ($d_i \geq 1$). Below we will define also $V_{i,j}$ ($j = 1, \ldots, d_i$), to be the Boolean variables associated to the multi-level variable V_i.

2.1 From discrete to Boolean models

Boolean (purely binary) and discrete (multi-level) models are related in several ways. One way to generate a Boolean model from a multi-level model is to generate a set of Boolean variables for each multi-level discrete variable (see, for instance, [16, 12, 13]). Our construction (detailed in the Appendix 1) is based on hypothesis H1.

Consider a discrete model $\Sigma_d = (\Omega_d, F_d)$, with variables $V = (V_1, \ldots, V_n)$, state space $\Omega_d = \{0, 1, \ldots, d_1\} \times \cdots \times \{0, 1, \ldots, d_n\}$, and a map $F_d : \Omega_d \to \Omega_d$ which defines the state transition table. This map lists all the possible transitions from each

state, and thus defines the possible dynamical trajectories of the system. At each state $V \in \Omega_d$, the next possible value for variable i is given by: $V_i^+ = (F_d)_i(V)$. Throughout this paper we will consider only *asynchronous dynamics*, where exactly one variable is updated at any given time (for more details, see Appendix 1). This gives rise to a non-deterministic system, where each state may have more than one successor:

$$V^+ \in \{W \in \Omega_d : \exists k \text{ s.t. } W_k = (F_d)_k(V) \neq V_k \text{ and } W_j = V_j,\ \forall j \neq k\}. \qquad (1)$$

Following previous work on multi-level systems [12, 13], it will be assumed that the state transition map F_d satisfies the hypothesis:

H1. Each variable V_i can only switch from its current level to an immediately adjacent level, that is:

$$V_i^+ \in \{V_i - 1, V_i, V_i + 1\},\ \ \forall i.$$

In other words, any variable V_i can only be increased or decreased by one unit at each time. This hypothesis represents the continuity of the biological variables: the concentration of a given protein cannot evolve from level d to level $d + 2$ without passing through level $d + 1$.

To construct a Boolean model Σ_b associated to Σ_d, the state space will be expanded by adding extra variables. If a discrete variable V_m takes values in the set $\{0, 1, \ldots, d_m\}$, then, in the Boolean model, d_m variables will be created (see [16, 12, 13]):

H2. For each $V_m \in \{0, 1, \ldots, d_m\}$ in the discrete model, generate $V_{m,1}, \ldots, V_{m,d_m} \in \{0, 1\}$ such that:

$$V_m = k \ \Leftrightarrow\ [\, V_{m,1} = \cdots = V_{m,k} = 1 \text{ and } V_{m,k+1} = \cdots = V_{m,d_m} = 0\,].$$

In particular, note that $V_{m,k} \geq V_{m,k+1}$, for all $k = 1, \ldots, d_m - 1$, meaning that if V_m is at a certain level, then all inferior levels must be "filled" as well. This hypothesis requires special attention when constructing the Boolean model from the discrete one, since we will wish to avoid transitions from a *permissible* (i.e., satisfying H2) to a *forbidden* (i.e., not satisfying H2) state. Our procedure deals with this problem in a natural way (see Appendix 1), and guarantees that no transitions from permissible to forbidden states take place.

2.2 From piecewise affine to multi-level discrete models

In models of genetic regulatory networks it is common to represent the activation (or inhibition) of one gene by another by a Heaviside function, that is, if the concentration of the first "gene" is below a certain threshold, then there is no transcription of the second gene; while above that threshold transcription is fully turned on. This description gives rise to *piecewise affine differential models* [6, 5]. A general way to represent the influence of variable x_i on variable x_k is through a step function with threshold θ_i^*. Increasing or decreasing step functions are defined as [6, 5]:

$$s^+(x_i, \theta_i^*) = \begin{cases} 0, & x_i < \theta_i^* \\ 1, & x_i > \theta_i^*, \end{cases}$$

and $s^-(x_i, \theta_i^*) = 1 - s^+(x_i, \theta_i^*)$[1]. These functions are not defined at the threshold points. At these points, the system of equations is defined as a differential inclusion [7, 2]. To construct a multi-level discrete model from the PWA model, based on the work [13], we will consider that the number of levels of a given variable x_i, is equal to the number of thresholds which define the influence of x_i on the other variables:

$$0 < \theta_i^1 < \theta_i^2 < \cdots < \theta_i^{d_i} < +\infty.$$

Define the corresponding multi-level discrete variable by:

$$V_i = \begin{cases} 0, & 0 \leq x_i \leq \theta_i^1 \\ k, & \theta_i^k < x_i \leq \theta_i^{k+1}, \ \ k = 1, \ldots, d_i - 1 \\ d_i, & \theta_i^{d_i} < x_i < +\infty. \end{cases} \tag{2}$$

To obtain a transition table (F_d) for the discrete model, the ordering among thresholds is used. Let V_i and V_i^+ denote, respectively, the discrete current and updated values for the continuous variable x_i. Suppose the level set of variable i is $\{0, 1, \ldots, d_i\}$. For each discrete combination of values (a vector $V = (V_1, \ldots, V_n) \in \Omega_d$), each continuous variable is in an interval between thresholds, as defined in (2). The PWA equation for x_i will take a particular expression for each V (see (6)-(9), for an example), and have a corresponding fixed (or focal) point $\hat{x} = \hat{x}(V)$. Then V_i is updated to evolve towards $\hat{x}_i$, in such a way that hypothesis H1 is satisfied: if $\hat{x}_i$ is in the interval $(\theta_i^k, \theta_i^{k+1})$, then

$$V_i^+ = (F_d)_i(V) \begin{cases} \min\{d_i, V_i + 1\}, & V_i < k, \\ V_i, & V_i = k, \\ \max\{0, V_i - 1\}, & V_i > k. \end{cases} \tag{3}$$

The state transition table F_d for the discrete system associated to the PWA system can thus be built. The discrete system evolves according to an asynchronous strategy, following the updating rule (1).

3 Example: the carbon starvation response in *E.coli*

As an example, the *E. coli* model developed by Ropers *et al.* in [10] and studied in [8] will be analysed (see these two references for more details on the biological and modelling aspects). This model describes the dynamics of a family of genes that regulate the carbon starvation response in *E.coli* (Fig. 1): *crp* (x_c), *cya* (x_y), *fis* (x_f), *gyrAB* (x_g), *topA* (x_t), and *rrn* (x_r). Nutritional stress is represented by an input $u \in \{0, 1\}$: $u = 0$ if carbon is present, and $u = 1$ in the absence of carbon.

3.1 Piecewise affine and discrete models

We will use the notation: $x = (x_c, x_y, x_f, x_g, x_t)' \in \mathbb{R}^5_{\geq 0}$ denotes the continuous variables, $V = (C, Y, F, G, T)' \in \Omega_d$ denotes the corresponding multi-level discrete variables, and C_i, $i = 1, \ldots, d_c$ denote the Boolean variables, associated with *crp*

[1] The superscripts "+" or "-" indicate whether the step function is increasing or decreasing. This notation is not related to V^+ used in discrete and Boolean systems, which designates the successor of state V. Since s^+ and V^+ are used for different systems (respectively, PWA and discrete), the notations will not be confused.

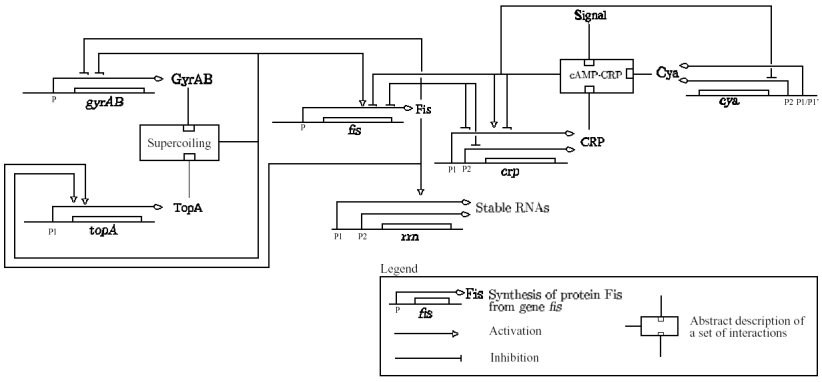

Figure 1: Genetic network, including proteins and regulations that come into play during a nutritional stress response in *E.coli*: CRP activation module (Cya, CRP, Fis), DNA Topology module (GyrAB, TopA, Fis), stable RNA output module (Rrn).

(similar notation is used for the other network components). The PWA equations are taken from [10]:

$$\begin{aligned}
\dot{x}_c &= \kappa_c^1 + \kappa_c^2 s^-(x_f,\theta_f^2)s^+(x_c,\theta_c^1)s^+(x_y,\theta_y^1)s^+(u,\theta_u) + \kappa_c^3 s^-(x_f,\theta_f^1) - \gamma_c x_c \\
\dot{x}_y &= \kappa_y^1 + \kappa_y^2[1 - s^+(x_c,\theta_c^3)s^+(x_y,\theta_y^3)s^+(u,\theta_u)] - \gamma_y x_y \\
\dot{x}_f &= \kappa_f^1[1 - s^+(x_c,\theta_c^1)s^+(x_y,\theta_y^1)s^+(u,\theta_u)]s^-(x_f,\theta_f^5) \\
&\quad + \kappa_f^2 s^+(x_g,\theta_g^1)s^-(x_t,\theta_t^2)s^-(x_f,\theta_f^5) \times [1 - s^+(x_c,\theta_c^1)s^+(x_y,\theta_y^1)s^+(u,\theta_u)] - \gamma_f x_f \\
\dot{x}_g &= \kappa_g^1[1 - s^+(x_g,\theta_g^2)s^-(x_t,\theta_t^1)]s^-(x_f,\theta_f^4) - \gamma_g x_g \\
\dot{x}_t &= \kappa_t^1 s^+(x_g,\theta_g^2)s^-(x_t,\theta_t^1)s^+(x_f,\theta_f^4) - \gamma_t x_t \\
\dot{x}_r &= \kappa_r^1 s^+(x_f,\theta_f^3) + \kappa_r^2 - \gamma_r x_r
\end{aligned} \tag{4}$$

with the following inequalities among thresholds:

$$\begin{aligned}
&0 < \theta_c^1 < \frac{\kappa_c^1}{\gamma_c} < \frac{\kappa_c^1 + \kappa_c^2}{\gamma_c} < \theta_c^2 < \theta_c^3 < \frac{\kappa_c^1 + \kappa_c^3}{\gamma_c} \\
&0 < \theta_y^1 < \frac{\kappa_y^1}{\gamma_y} < \theta_y^2 < \theta_y^3 < \frac{\kappa_y^1 + \kappa_y^2}{\gamma_y} \\
&0 < \theta_f^1 < \frac{\kappa_f^1}{\gamma_f} < \theta_f^2 < \theta_f^3 < \theta_f^4 < \theta_f^5 < \frac{\kappa_f^1 + \kappa_f^2}{\gamma_f} \\
&0 < \theta_g^1 < \theta_g^2 < \frac{\kappa_g}{\gamma_g} \\
&0 < \theta_t^1 < \theta_t^2 < \frac{\kappa_t}{\gamma_t}
\end{aligned} \tag{5}$$

To construct a discrete (multi-level) system from (4), note that:

- *crp* contributes to inhibit *fis* and activate itself once it reaches threshold θ_c^1, and contributes to *cya* inhibition at θ_c^3. Since threshold θ_c^2 doesn't enter into any equations, it will not be considered here;

- *cya* contributes to inhibit *fis* and activate *crp* at θ_y^1 and contributes to its own inhibition at θ_y^3. As for *crp*, the level θ_y^2 will not be considered here;
- *gyrAB* contributes to *fis* activation at θ_g^1, and inhibits itself and activates *topA* at θ_g^2;
- *topA* influences *gyrAB* and inhibits itself at θ_t^1 and contributes to *fis* inhibition at θ_t^2;
- *fis* has five threshold concentrations. It inhibits *crp* promoters 1 and 2 once it reaches lower thresholds θ_f^1 and θ_f^2, activates *rrn* at threshold θ_f^3, inhibits gyrAB and activates topA at θ_f^4, and inhibits itself at θ_f^5.

Since *rrn* is an output variable (it doesn't influence any of the other five), we will drop this variable and consider only four different thresholds for *fis*. Without loss of generality for the dynamics of the model, one can also say that *rrn* is activated once *fis* is above θ_f^2 (or θ_f^4). Therefore, we will assume that: $C, Y, G, T \in \{0, 1, 2\}$ and $F \in \{0, 1, \ldots, 4\}$.

To obtain the discrete model from equations (4), we follow the method indicated above. For example, consider the equation for x_c, which can take only one of four forms:

$$\dot{x}_c = \kappa_c^1 - \gamma_c x_c \quad (6)$$
$$\dot{x}_c = \kappa_c^1 + \kappa_c^2 - \gamma_c x_c \quad (7)$$
$$\dot{x}_c = \kappa_c^1 + \kappa_c^3 - \gamma_c x_c. \quad (8)$$
$$\dot{x}_c = \kappa_c^1 + \kappa_c^2 + \kappa_c^3 - \gamma_c x_c \quad (9)$$

Let C and C^+ denote, respectively, the current and updated value for variable *crp*. For any state $V \in \Omega_d$, consider the appropriate equation (6)-(9), together with inequalities (5). In cases (6), (7): $C^+ = C+1$ if $C = 0$, $C^+ = C$ if $C = 1$, and $C^+ = C-1$ if $C = 2$. In cases (8), (9): $C^+ = C+1$ if $C < 2$, and $C^+ = C$ if $C = 2$. The multi-level discrete model obtained from the PWA model is represented by its transition tables in the Appendices 2-5.

3.2 Boolean model

Following the method described in Section 2.1, and from the Tables in the Appendices 2-5, the Boolean model for the *E. coli* network can be written:

$$\begin{aligned}
U^+ &= U \\
C_1^+ &= 1 \\
C_2^+ &= (\overline{U} \wedge C_1 \wedge \overline{F_1}) \vee (U \wedge C_1 \wedge \overline{F_2} \wedge \overline{F_3} \wedge \overline{F_4}) \\
Y_1^+ &= 1 \\
Y_2^+ &= (\overline{U} \wedge Y_1) \vee (U \wedge [(Y_1 \wedge (\overline{C_1} \vee \overline{C_2})) \vee ((Y_1 \wedge \overline{Y_2}) \wedge C_1 \wedge C_2)]) \\
G_1^+ &= (\overline{F_3} \wedge \overline{F_4}) \vee [(F_1 \wedge F_2 \wedge F_3) \vee G_2] \\
G_2^+ &= \overline{F_3} \wedge \overline{F_4} \wedge G_1 \wedge (\overline{G_2} \vee T_1 \vee T_2) \\
T_1^+ &= [\overline{F_3} \wedge \overline{F_4} \wedge T_2] \vee [F_1 \wedge F_2 \wedge F_3 \wedge ((\overline{G_2} \wedge T_2) \vee (G_2 \wedge (T_2 \vee \overline{T_1})))] \\
T_2^+ &= 0 \\
F_1^+ &= (\overline{U} \wedge H_1^0) \vee (U \wedge H_1^1) \\
F_2^+ &= (\overline{U} \wedge H_2^0) \vee (U \wedge H_2^1) \\
F_3^+ &= (\overline{U} \wedge H_3^0) \vee (U \wedge H_3^1) \\
F_4^+ &= (\overline{U} \wedge H_4^0) \vee (U \wedge H_4^1)
\end{aligned}$$

Table 1: Attractors of Boolean model.

Att.	C_1	C_2	Y_1	Y_2	G_1	G_2	T_1	T_2	F_1	F_2	F_3	F_4
A1 ($U=1$)	1	1	1	$*$	1	$*$	0	0	0	0	0	0
A0 ($U=0$)	1	0	1	1	$*$	$*$	$*$	0	1	$*$	$*$	$*$

where:

$$
\begin{aligned}
H_1^0 &= 1 \\
H_2^0 &= (F_1 \wedge G_1 \wedge \overline{T_2}) \vee (F_1 \wedge F_2 \wedge F_3) \\
H_3^0 &= (F_1 \wedge F_2 \wedge G_1 \wedge \overline{T_2}) \vee (F_1 \wedge F_2 \wedge F_3 \wedge F_4) \\
H_4^0 &= (F_1 \wedge F_2 \wedge F_3 \wedge \overline{F_4} \wedge G_1 \wedge \overline{T_2}) \\
H_1^1 &= [((\overline{C_1} \wedge \overline{C_2}) \vee (\overline{Y_1} \wedge \overline{Y_2})) \wedge H_1^0] \vee [(C_1 \vee C_2 \vee Y_1 \vee Y_2) \wedge F_1 \wedge F_2] \\
H_2^1 &= [((\overline{C_1} \wedge \overline{C_2}) \vee (\overline{Y_1} \wedge \overline{Y_2})) \wedge H_2^0] \vee [(C_1 \vee C_2 \vee Y_1 \vee Y_2) \wedge F_1 \wedge F_2 \wedge F_3] \\
H_3^1 &= [((\overline{C_1} \wedge \overline{C_2}) \vee (\overline{Y_1} \wedge \overline{Y_2})) \wedge H_3^0] \vee [(C_1 \vee C_2 \vee Y_1 \vee Y_2) \wedge F_1 \wedge F_2 \wedge F_3 \wedge F_4] \\
H_4^1 &= [((\overline{C_1} \wedge \overline{C_2}) \vee (\overline{Y_1} \wedge \overline{Y_2})) \wedge H_4^0].
\end{aligned}
$$

Analysis of this Boolean model (using the computational tools described in [14]) shows that it has two attractors: a strongly connected component with four states when $U = 1$, and a strongly connected component with 24 states in the case $U = 0$. In Table 1, the fixed coordinates for each attractor are indicated. Following the method used in [14], it is possible to computationally identify the "operational interactions" within this attractor, and the variables associated with these interactions. That will give a subsystem of the original system.

For attractor A1 ($U = 1$), we obtain: $G_2^+ = \overline{G_2}$ and $Y_2^+ = \overline{Y_2}$. That is, keeping one of the two variables G_2 or Y_2 fixed, the other can switch between zero and one, generating a fully reversible cycle as shown in Fig. 3 (see interpretation in Section 5).

For the attractor A0 ($U = 0$), the operational subnetwork is depicted in Fig. 2. The diagram of interactions corresponding to this reduced system is shown in Fig. 2. Several cycles are possible within attractor A0. The corresponding transition graph is

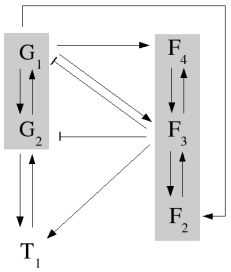

$$
\begin{aligned}
G_1^+ &= \overline{F_3} \vee G_2 \\
G_2^+ &= \overline{F_3} \wedge G_1 \wedge (\overline{G_2} \vee T_1) \\
T_1^+ &= F_3 \wedge G_2 \wedge \overline{T_1} \\
F_2^+ &= G_1 \vee F_3 \\
F_3^+ &= (G_1 \vee F_4) \wedge F_2 \\
F_4^+ &= G_1 \wedge F_3 \wedge \overline{F_4}.
\end{aligned}
$$

Figure 2: Operational interactions within attractor A0. Shaded regions indicate Boolean variables related to the same discrete multi-valued variable.

represented in Figs. 5 ($T_1 = 0$) and 6 ($T_1 = 1$), and discussed in Section 4.

4 Comparison between Boolean and PWA differential models

To compare the two modelling formalisms, we now briefly summarize the results obtained in [8] for the model (4). First, the solutions were defined with the help of Filippov's differential inclusions. Then, the asymptotic dynamics were computed for the two values of the input. This system exhibits both equilibria (some in the sense of Filippov) and sliding modes (stable sliding motion along a threshold).

For the case $U = 1$, the asymptotic dynamics of (4) satisfies:

- $x_c(t) \to \frac{\kappa_c^1+\kappa_c^2+\kappa_c^3}{\gamma_c} > \theta_c^3 > \theta_c^2$;
- $x_y(t) = \theta_y^3$, in finite time;
- $x_f(t) \to 0$;
- $x_g(t) = \theta_g^2$, in finite time;
- $x_t(t) \to 0$.

Therefore, the solutions converge to a fixed point in the sense of Filippov. In practice, one may expect a sliding mode along $x_g = \theta_g^2$, and "chattering" in the variable x_g. Variable x_y satisfies a similar dynamics. This characterization is obtained also with the Boolean model which, for the case $U = 1$, converges to an attractor with four states (Fig. 3). In these states only the values of $G_2 \in \{0, 1\}$ and $Y_2 \in \{0, 1\}$ may vary,

$$\begin{array}{ccc} 00 & \leftrightarrows & 1{:}0 \\ \downarrow\uparrow & & \downarrow\uparrow \\ 0{:}1 & \leftrightarrows & 1{:}1 \end{array}$$

Figure 3: Transition graph within attractor A1.The state 1:0 represents: $(G_2, Y_2) = (1, 0)$.

and the transitions indeed correspond to a chattering mode in the variables x_g and/or x_y, between the highest ($G_1 = G_2 = 1$ or $Y_1 = Y_2 = 1$) and intermediate ($G_1 = 1$, $G_2 = 0$ or $Y_1 = 1$, $Y_2 = 0$) levels. The variables $C_1 = C_2 = 1$ indicate that x_c converges to its highest level, and also $T_{1,2} = 0$, $F_{1,2,3,4} = 0$, exactly recovering the piecewise affine asymptotic results for x_t and x_f.

For the case $U = 0$, the asymptotic dynamics of (4) can be reduced to the equations on x_g and x_f (see Fig. 4) with:

- $x_c(t) \to \frac{\kappa_c^1}{\gamma_c}$ and $x_y(t) \to \frac{\kappa_y^1+\kappa_y^2}{\gamma_y}$, after some finite time;
- $x_t(t) \leq \theta_t^1$ and $x_g(t) \leq \theta_g^2$, after some finite time;
- Sliding mode along the plane $x_t = \theta_t^1$ with the solution eventually jumping down to the region $x_t < \theta_t^1$, and staying there;
- Sliding mode along the line $x_g = \theta_g^2$ and $x_f < \theta_f^4$, with the solution reaching (and leaving) the point $x_g = \theta_g^2$ and $x_f = \theta_f^4$ in finite time;

- Sliding mode along the line $x_g > \theta_g^1$ and $x_f = \theta_f^5$, with the solution reaching (and leaving) the point $x_g = \theta_g^1$ and $x_f = \theta_f^5$ in finite time;
- Damped oscillations around the point $x_g = \theta_g^1$ and $x_f = \theta_f^4$. It is shown that all trajectories will asymptotically converge to this point, which is an equilibrium in the sense of Filippov.

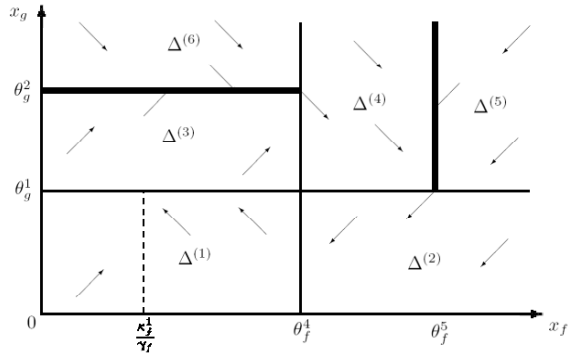

Figure 4: Asymptotic behaviour of (4) in the (x_f, x_g) plane, for the case $U = 0$. Thick black lines indicate sliding modes (cf [8]).

In this case, the interaction graph of the asymptotic system (x_f, x_g, x_t) obtained in [8] (see also the diagram analysis in [15]), is recovered in the diagram of operational interactions in Fig. 2. The same interaction graph is obtained, with one negative loop between G and F, and two positive loops of length 2 and 3. The Boolean model correctly predicts the levels for x_c (intermediate, with $C_1 = 1$, $C_2 = 0$) and x_y (highest, with $Y_1 = 1$, $Y_2 = 1$). The Boolean model also predicts the three sliding modes: the transitions between states 000:110⇋000:100 or 100:110⇋100:100 (Table 5), describe a possible chattering behaviour in variable G, which recovers the sliding mode along the line $x_g = \theta_g^2$. Similarly, the sliding mode along $x_f = \theta_f^5$, is also recovered, with the transitions between states 110:110⇋111:110 or 110:100⇋111:100. Finally, from every state with $T_1 = 1$, a transition is possible to the corresponding state with the same Boolean values but for $T_1 = 0$, i.e.: abc.de1→abc.de0. This transition is possible in both senses for the states: 110:111⇋110:110 and 111:111⇋111:110 (states marked with $*$) (see Tables 5 and 6). This captures the fact that eventually $x_t \leq \theta_t^1$, together with the sliding mode along $x_t = \theta_t^1$. For the oscillations in x_f, x_g, the Boolean model predicts the same orientation as that of the PWA model (compare Figs. 5 and 4). Note that these figures can be read as a "phase portrait" of the system, with the period two oscillations corresponding to the dark solid lines in Fig. 4.

In summary, all the main qualitative asymptotic properties of the PWA system are recovered in its Boolean counterpart. Nevertheless, one should note that, given the exclusively qualitative nature of Boolean networks, some fine-grained aspects of the dynamics are lost. In the previous example, even though the phase portraits of both systems are identical from a qualitative point of view, the Boolean model loses the fact that the oscillations are damped, and eventually converges towards a singular steady state. In [8], the demonstration of this convergence was made through a fine analysis of the sliding modes, based on Filippov theory. The Boolean model also looses the

$$\begin{array}{ccccccc} 000{:}110 & \rightarrow & 100{:}110 & \rightarrow & 110{:}110^* & \leftrightarrows & 111{:}110^* \\ \downarrow\uparrow & & \downarrow\uparrow & & \downarrow & & \downarrow \\ 000{:}100 & \rightarrow & 100{:}100 & \rightarrow & 110{:}100 & \leftrightarrows & 111{:}100 \\ \uparrow & & \uparrow & & \downarrow & & \downarrow \\ 000{:}000 & \leftarrow & 100{:}000 & \leftarrow & 110{:}000 & \leftarrow & 111{:}000 \end{array}$$

Figure 5: Transition graph within attractor A0, case $T_1 = 0$. The state 110:100 represents: $(F_2, F_3, F_4) = (1, 1, 0)$ and $(G_1, G_2, T_1) = (1, 0, 0)$. The star indicates a possible transition to the corresponding state with $T_1 = 1$.

$$\begin{array}{ccccccc} 000{:}111^* & \rightarrow & 100{:}111^* & \rightarrow & 110{:}111^* & \leftrightarrows & 111{:}111^* \\ \uparrow & & \uparrow & & \downarrow & & \downarrow \\ 000{:}101^* & \rightarrow & 100{:}101^* & \rightarrow & 110{:}101^* & \leftrightarrows & 111{:}101^* \\ \uparrow & & \uparrow & & \downarrow & & \downarrow \\ 000{:}001^* & \leftarrow & 100{:}001^* & \leftarrow & 110{:}001^* & \leftarrow & 111{:}001^* \end{array}$$

Figure 6: Transition graph within attractor A0, case $T_1 = 1$. The state 110:101 represents: $(F_2, F_3, F_4) = (1, 1, 0)$ and $(G_1, G_2, T_1) = (1, 0, 1)$. The star indicates a possible transition to the corresponding state with $T_1 = 0$.

information that the lines $x_g = \theta_g^2$ or $x_f = \theta_f^5$ (bold lines in Fig. 4) are in fact "black walls", which effectivelly prevent trajectories to cross from one side to the other. This information is, however, only hidden in the Boolean framework and can be uncovered by finer modelling, to recover the convergence towards singular domains. This will be shown next, for a simple example.

5 Sliding modes and period two Boolean oscillations

The attractors of a Boolean model describe the possible asymptotic behaviours of the network and depend on the model's size, connectivity, and rules. The attractors in a given network can be counted and classified according to its qualitative dynamical properties [1] but, however, not all attractors represent biologically relevant or even observed behaviour. In our example, we observe several short one-step cycles where the system may be locked in a period 2 oscillation that might constitute suspicious non-biological behaviour. Nevertheless, in this case, comparison with the PWA model shows that *all the one-step oscillations* correspond to a given "sliding mode" in the continuous system. The biological significance of these sliding motions can be related to the phenomenon of homeostasis, where the regulatory network contributes to maintain a biological species around a given level.

Assume that the Boolean model dynamics has a period 2 oscillation in variable i, whenever the system is in a subset $R^b \in \Omega$:

$$X_i^+ = F_i(X) = \overline{X_i} = \begin{cases} 0, & X_i = 1,\ X \in R^b \\ 1, & X_i = 0,\ X \in R^b. \end{cases} \tag{10}$$

The smallest possible set $R^b = \{X^0, X^1\}$, is such that $X_i^0 = 0 = 1 - X_i^1$, and $X_j^0 = X_j^1$ for all $j \neq i$. Following our rules for construction of Boolean models, $X_i = 1$ (resp., $X_i = 0$) means that $x_i > \theta_i$, (resp., $x_i \leq \theta_i$). We will consider that

each Boolean variable corresponds to one continuous variable (only one threshold per variable): one can restrict the system to a region in the state space where only x_i has a threshold value, and all other x_j are in a interval between two thresholds. According to (3), the focal point $\hat{x}_i$ (computed from $f_i(\hat{x}) = 0$) for the x_i equation must satisfy:

$$\begin{aligned} x_i > \theta_i \text{ and } X_i^+ = \overline{X_i}: &\quad \hat{x}_i < \theta_i \\ x_i < \theta_i \text{ and } X_i^+ = \overline{X_i}: &\quad \hat{x}_i > \theta_i, \end{aligned}$$

that is, the PWA equation for x_i must satisfy:

$$\dot{x}_i = f_i(x) \begin{cases} < 0, & x_i > \theta_i, x \in R \\ \text{any}, & x_i = \theta_i, x \in R \\ > 0, & x_i < \theta_i, x \in R \end{cases}$$

where

$$R = \{x \in \mathbb{R}^n_{\geq 0} : \text{sign}(X_j - 1/2)x_j > \theta_j,\ \theta_i - \varepsilon < x_i < \theta_i + \varepsilon\}$$

that is, each x_j is above or below its threshold depending on the value of the corresponding Boolean variable X_j, while x_i is the only one that may range over an interval containing its threshold. Thus, on R, sign$(f_j(x))$ =const., for all $x \in R$, $j \neq i$.

Since the sign of the vector field of variable i depends only on itself, the simplest PWA system that satisfies these properties is of the form

$$\begin{aligned} \dot{x}_i &= f_i(x) = \kappa_i s^-(x_i, \theta_i) - \gamma_i x_i, \quad x \in R, \\ \dot{x}_j &= f_j(x), \quad \text{has constant sign } \forall\, x \in R \quad (j \neq i) \end{aligned}$$

with a negative auto-regulatory function for i, and $\theta_i < \kappa_i/\gamma_i$. By assumption, x_i is the first variable to reach a threshold, and we observe that the equation for x_i (in R) is decoupled from the rest of the system and can be analyzed separately. The equation for x_i admits no equilibrium with $x_i \neq \theta_i$ (since $f_i(x) \neq 0$), but it admits an equilibrium of Filippov type satisfying: $\hat{x}_i = \theta_i$. This gives rise to a "sliding mode" solution on R, where x_i reaches θ_i in finite time and the other variables strictly increase or decrease until the boundary of R is reached. If the system suffers a small perturbation on x_i, it will respond by again converging towards θ_i. In theory, we expect no oscillations in x_i, even if, due to the discontinuity in the vector field, numerical simulations may show oscillations. For the 1-dimensional system $\dot{x}_i = \kappa_i s^-(x_i, \theta_i) - \gamma_i x_i$ a comparison can be made with the solution of a continuous vector field $\dot{x}_i = \kappa_i \frac{\theta_i^p}{\theta_i^p + x_i^p} - \gamma_i x_i$ ($p \geq 2$), which has a single stable equilibrium, and no damped oscillations. In the current Boolean model, there are not enough variables to represent a solution with fixed $x_i = \theta_i$, so the discrete solution converges to an attractor comprising both states X^0 and X^1 which are equally "close" to the state $x_i = \theta_i$.

In fact, this correspondence between period 2 oscillations and sliding modes can be further interpreted as follows: the "back-and-forth' oscillatory behaviour may be the result of the existence of an intermediate variable which is lacking in the Boolean model. So, introduce a new variable associated with x_i as follows:

$$X_{i*} = \begin{cases} 0, & x_i < \theta_i \\ 1, & x_i \geq \theta_i. \end{cases}$$

Then we have

$$\begin{aligned} x_i < \theta_i &\Leftrightarrow X_{i*} = X_i = 0 \\ x_i = \theta_i &\Leftrightarrow X_{i*} = 1,\ X_i = 0 \\ x_i > \theta_i &\Leftrightarrow X_{i*} = X_i = 1. \end{aligned}$$

In order to define the Boolean dynamics, we construct the following table:

x_i	X_{i*}	X_i	X_{i*}^+	X_i^+
$< \theta_i$	0	0	1	0
$= \theta_i$	1	0	1	0
$> \theta_i$	1	1	1	0

The first and third line are straightforward. The second line is interpreted like this: when $(X_{i*}, X_i) = (1, 0)$, i.e. when $x_i = \theta_i$, then the two neighbor vector fields are of opposite sign, and therefore force the variable x_i to remain constant.

To illustrate this, consider the attractor A1 (Fig. 3), consisting of the reversible transitions in a 2 dimensional space G_2Y_2. Note that, fixing either of the variables, the other may have a period 2 oscillation. Introducing one intermediate variable for each of G_2 and Y_2, the attractor A1 expands to (with notation $G_{2*}G_2 : Y_{2*}Y_2$):

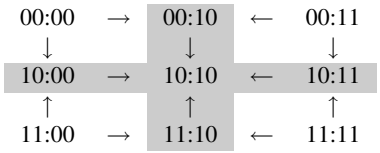

This diagram represents exactly the Filippov type equilibrium for the case $U = 1$, where $x_g \to \theta_g^2$ and $x_y \to \theta_y^3$ in finite time. In the Boolean model, both one-step oscillations disappear, and the strongly connected component containing four states is "decoupled", giving rise to a Boolean steady state: $G_{2*}^+ = 1$, $G_2^+ = 0$, $Y_{2*}^+ = 1$, and $Y_2^+ = 0$.

6 Conclusions

A comparison between two formalisms, Boolean and piecewise affine models, was explored in this paper. It was verified that the Boolean model captures most of the asymptotic behaviour of the system, even though the PWA model gives more details. Namely, while the Boolean model correctly reproduces oscillatory behaviour and sliding modes, it cannot capture convergence to a given point through damped oscillations, or the fact that a sliding mode along a given line plays the role of a black wall. This latter problem can be circumvented by noticing that there is a correspondence between sliding modes and period 2 Boolean cycles, and adding a new variable to more finely describe the local oscillatory behaviour. Therefore, dynamical behaviour in the Boolean model that might be considered as non-relevant biologically may in fact contain useful information for analysis of complex systems.

Moreover, for the *E. coli* network, we have been able to identify a Boolean subsystem corresponding to each attractor of the full Boolean system. In our case, the dynamics of this asymptotic Boolean system was compared to the computed asymptotic dynamics of the differential system, and shown to be very similar. More generally, this reduced Boolean asymptotic system could be again translated into a continuous one, to obtain a reduced system of the full differential system, hopefully keeping some of the asymptotic properties of the full system. This offers interesting perspectives for model reduction.

Given the available computational tools for Boolean analysis, based on well known and efficient graph algorithms (see, for instance, [11, 10, 14]), the construction of a Boolean model associated to a PWA system can therefore constitute an undeniable help for the analysis of genetic regulatory networks.

7 Acknowledgments

This work was supported in part by the French National Research Agency through the BioSys project MetaGenoReg.

References

[1] R.J. Bagley and L. Glass. Counting and classifying attractors in high dimensional dynamical systems. *J. Theor. Biol.*, 183:269–284, 1996.

[2] R. Casey, H. de Jong, and J.L. Gouzé. Piecewise linear models of genetic regulatory networks: equilibria and their stability. *J. Math. Biol.*, 52:27–56, 2006.

[3] M. Chaves, T. Eißing, and F. Allgöwer. Regulation of apoptosis via the nfkb pathway: modeling and analysis. In A. Deutsch N. Ganguly and A. Mukherjee, editors, *Dynamics on and of complex networks: applications to biology, computer science and the social sciences*, Modeling and Simulation in Science, Engineering and Technology, pages 19–34. Birkhauser, Boston, 2009.

[4] M. Chaves, E.D. Sontag, and R. Albert. Methods of robustness analysis for boolean models of gene control networks. *IEE Proc. Systems Biology*, 235:154–167, 2006.

[5] L. Glass. Classification of biological networks by their qualitative dynamics. *J. Theor. Biol.*, 54:85–107, 1975.

[6] L. Glass and S.A. Kauffman. The logical analysis of continuous, nonlinear biochemical control networks. *J. Theor. Biol.*, 39:103–129, 1973.

[7] J.L. Gouzé and T. Sari. A class of piecewise linear differential equations arising in biological models. *Dyn. Syst.*, 17(4):299–316, 2002.

[8] F. Grognard, J.-L. Gouzé, and H. de Jong. Piecewise-linear models of genetic regulatory networks: theory and example. In I. Queinnec, S. Tarbouriech, G. Garcia, and S. Niculescu, editors, *Biology and control theory: current challenges*, Lecture Notes in Control and Information Sciences (LNCIS) 357, pages 137–159. Springer-Verlag, 2007.

[9] S. Liang, S. Fuhrman, and R. Somogyi. REVEAL, a general reverse engineering algorithm for inference of genetic network architecture. In *Pacific Symposium on Biocomputing*, volume 3, pages 18–29, 1998.

[10] D. Ropers, H. de Jong, M. Page, D. Schneider, and J. Geiselmann. Qualitative simulation of the carbon starvation response in *Escherichia coli*. *Biosystems*, 84(2):124–152, 2006.

[11] L. Sánchez and D. Thieffry. A logical analysis of the *Drosophila* gap-gene system. *J. Theor. Biol.*, 211:115–141, 2001.

[12] E.H. Snoussi and R. Thomas. Logical identification of all steady states: the concept of feedback loop characteristic states. *Bull. Math. Biol.*, 55(5):973–991, 1993.

[13] R. Thomas and R. D'Ari. *Biological feedback*. CRC Press, 1990.

[14] L. Tournier and M. Chaves. Uncovering operational interactions in genetic networks using asynchronous boolean dynamics. *J. Theor. Biol.*, 260(2):196–209, 2009.

[15] L. Tournier and J.-L. Gouzé. Hierarchical analysis of piecewise affine models of gene regulatory networks. *Theory Biosci.*, 127:125–134, 2008.

[16] P. van Ham. How to deal with more than two levels. In R. Thomas, editor, *Kinetic Logic: A Boolean Approach to the Analysis of Complex Regulatory Systems*, volume 29 of *Lecture Notes in Biomathematics*, pages 326–343. Springer, 1979.

[17] G. von Dassow, E. Meir, E.M. Munro, and G.M. Odell. The segment polarity network is a robust developmental module. *Nature*, 406:188–192, 2000.

[18] J. Zhang, K.H. Johansson, J. Lygeros, and S. Sastry. Zeno hybrid systems. *Int. J. Robust Nonlinear Control*, 11:435–451, 2001.

APPENDICES

1 Discrete (multi-level) and Boolean

Here, an intuitive algorithm is proposed, and shown to always provide a biologically feasible model consistent with the multi-level one. Our construction is based on the hypothesis that each multi-level variable can only switch between adjacent level (see H1, below).

Consider a discrete model $\Sigma_d = (\Omega_d, F_{d,syn})$, with variables $V = (V_1, \ldots, V_M)$, state space $\Omega_d = \{0, 1, \ldots, d_1\} \times \cdots \times \{0, 1, \ldots, d_M\}$, and a map $F_{d,syn} : \Omega_d \to \Omega_d$ defining the state transition table. This map lists all the possible transitions from each state, and thus defines the possible dynamical trajectories of the system. At each state $V \in \Omega_d$, the next possible state for variable i is given by:

$$V_i^+ = (F_{d,syn})_i(V).$$

There are different strategies for updating a discrete system, leading to different dynamics. The synchronous algorithm consists of updating all variables simultaneously: $V^+ = F_{d,syn}(V)$ is called the *synchronous* successor of V. A more general and realistic dynamics can be obtained using an *asynchronous* updating algorithm, where exactly one variable is updated at any given time. In the asynchronous case we have:

$$V^+ = F_{d,asyn}(V)$$

where each state $V \in \Omega_d$ may have more than one asynchronous successor, in fact there are as many as the number of variables k that change value in the synchronous table:

$$F_{d,asyn}(V) \in \{W \in \Omega_d : W_k = (F_{d,syn})_k(V) \neq V_k, \text{ for some } k; \text{ and } W_i = V_i,\ i \neq k\}.$$

In particular, the asynchronous algorithm gives rise to a non-deterministic system, while the synchronous system is deterministic, since at each state only one successor exists.

Throughout this Section, we use the notation $F_{d,syn}$ to represent the state transition table and synchronous dynamics, and use

$$V[t+1] = F_{d,asyn}(V[t]). \tag{11}$$

to represent the asynchronous dynamics, where exactly one variable is updated at any given time.

Following the work in [16, 12, 13], it will be assumed that system Σ_d satisfies hypotheses H1 and H2.

H1. Each variable V_m can only switch from its current level to an immediately adjacent level, that is:

$$V_m^+ \in \{V_m - 1, V_m, V_m + 1\}.$$

In other words, any variable V_m can only be increased or decreased by one unit at each time.

To construct a Boolean model Σ_b associated to Σ_d, the state space will be formed by adding extra variables. If a discrete variable V_m takes values in the set $\{0, 1, \ldots, d_m\}$, then, in the Boolean model, d_m variables will be created:

H2. For each $V_m \in \{0, 1, \ldots, d_m\}$ in the discrete model, generate $V_{m,1}, \ldots, V_{m,d_m} \in \{0, 1\}$ such that:

$$\begin{aligned} V_m = k \quad \Leftrightarrow \qquad & V_{m,1} = \cdots = V_{m,k} = 1 \\ \text{and} \quad & V_{m,k+1} = \cdots = V_{m,d_m} = 0. \end{aligned} \tag{12}$$

In particular, note that $V_{m,k} \geq V_{m,k+1}$, for all $k = 1, \ldots, d$, meaning that if V_m is at a certain level, then all inferior levels must be "filled" as well.

More generally, if there are M discrete variables, each with d_m ($m = 1, \ldots, M$) levels, define: $D = (d_1, \ldots, d_M)$, $n = d_1 + \cdots + d_M$ and set $\Omega = \{0, 1\}^n$. Then define a function $\varphi_D : \Omega_d \to \Omega$, such that:

$$\varphi_D(V) = (V_{1,1}, \ldots, V_{1,d_1}, \ldots, V_{M,1}, \ldots, V_{M,d_M}), \tag{13}$$

where $V_{m,k}$ are defined as in (12). It is clear that the function is injective, but $\varphi_D(\Omega_d)$ is strictly contained in Ω. Namely, those elements of Ω that would satisfy $V_{m,k} < V_{m,k+1}$ for some m and some $1 \leq k \leq d_m$ do not have a pre-image in Ω_d. In fact, such combinations are biologically meaningless, in view of the interpretation of (12). Moreover, when constructing the Boolean rules for the extended system, one naturally wishes to avoid transitions to these unfeasible states, in order to obtain a biologically significant model. Define the sets of *permissible* and *forbidden* states of Ω, associated with D:

$$\begin{aligned} S_{D,p} = \quad & \{X \in \Omega : \ (\forall\, 1 \leq m \leq M)(\forall\, 1 \leq k \leq d_m),\ X_{m,k} \geq X_{m,k+1}\} \\ S_{D,f} = \quad & \{X \in \Omega : \ (\exists\, 1 \leq \bar{m} \leq M)(\exists\, 1 \leq \bar{k} \leq d_{\bar{m}}),\ X_{\bar{m},\bar{k}} < X_{\bar{m},\bar{k}+1}\}, \end{aligned}$$

where the n coordinates of vector $X \in \Omega$ are labelled in M groups of length d_m:

$$X = (X_{1,1}, \ldots, X_{1,d_1}, \ldots, X_{M,1}, \ldots, X_{M,d_M}). \tag{14}$$

Note that: $S_{D,p} = \varphi_D(\Omega_d), \quad S_{D,f} = \Omega \setminus S_{D,p}$, in view of H2. Then φ_D is a bijection between Ω_d and $S_{D,p}$, so it is possible to define a (partial) inverse function:

$$\varphi_{D,p}^{-1} : S_{D,p} \to \Omega_d, \quad \varphi_{D,p}^{-1}(X) = (V_1, \ldots, V_M),$$

where $V_m = \sum_k X_{m,k}$. An algorithm for generating a Boolean model $\Sigma_b = (D, \Omega, F_{b,syn})$ associated to Σ_d is then as follows:

1. Generate the state space: $\Omega = \{0,1\}^n$ with $n = d_1 + \cdots + d_M$, and label the coordinates of $X \in \Omega$ according to (14);
2. Translate the discrete value table $V^+ = F_{d,syn}(V)$ into a Boolean value table $X^+ = F_{b,syn}(X)$, for each $X \in S_{D,p}$:

   $$F_{b,syn}(X) := \varphi_D(F_{d,syn}(V)) = \varphi_D(F_{d,syn}(\varphi_{D,p}^{-1}(X)))$$

   (note that this assigns values to $X \in S_{D,p}$ only);
3. Complete the table $F_{b,syn}$ by assigning any function $\psi : \Omega \to \Omega$ to the Boolean states $X \in S_{D,f}$:

   $$F_{b,syn}(X) = \begin{cases} \varphi_D(F_{d,syn}(\varphi_{D,p}^{-1}(X))), & X \in S_{D,p} \\ \psi(X), & X \in S_{D,f}; \end{cases}$$

4. Obtain Boolean logical rules from the (now full) synchronous truth table $F_{b,syn}$.

Note that step 3 can be viewed as the identification of a n-dimensional Boolean map, verifying certain constraints (on the set $S_{D,p}$) and with some degrees of freedom (on the set $S_{D,f}$). Thus the map $F_{b,syn} : \Omega \to \Omega$ is not necessarily unique. To construct this map, one can use a reverse engineering algorithm, to find a function ψ according to some suitable criteria (for instance, REVEAL [9] will find a function ψ with minimal node connectivity). In any case, whatever $F_{b,syn}(S_{D,f})$ is, *it will not affect the dynamics of the biologically relevant part of the Boolean model* (cf. Lemma 1.1). An example of a multi-level to Boolean table translation can be seen in Table 2, for the *E. coli* example. A completed Boolean truth table is shown in Table 3, where the rows corresponding to forbidden states are shaded in grey.

The Boolean model thus obtained is well defined and consistent with the discrete model, in the sense that no forbidden state will be a successor of a permissible state. However, forbidden states can succeed one another or go into an permissible state. This means that, even though some parts of the state space will be biologically meaningless, it is guaranteed that once a trajectory enters the meaningful part ($S_{D,p}$) it will remain there.

For the Boolean model $\Sigma_b = (D, \Omega, F_{b,syn})$, one can also define an asynchronous dynamics from $F_{b,syn}$, by updating only one Boolean variable at a time:

$$X[t+1] = F_{b,asyn}(X[t]). \tag{15}$$

If $X^+ = F_{b,syn}(X) = X$ then also $X[t+1] = X[t]$ for all t, and X is called an equilibrium point.

Lemma 1.1 Suppose Σ_d is a multi-level system that satisfies H1. The Boolean system $\Sigma_b = (D, \Omega, F_{b,syn})$, constructed according to H2 and points 1 to 3, allows only transitions from $S_{D,p}$ or $S_{D,f}$ into $S_{D,p}$ or from $S_{D,f}$ into itself (for both synchronous and asynchronous updating strategies).

Proof: Given any $X \in S_{D,p}$, we want to show that $X^+ = F_{b,syn}(X) \in S_{D,p}$. By definition of $F_{b,syn}$, φ_D and $\varphi_{D,p}^{-1}$ we have:

$$F_{b,syn}(X) = \varphi_D(F_{d,syn}(\varphi_{D,p}^{-1}(X))) = \varphi_D(F_{d,syn}(V)) = \varphi_D(V^+),$$

for some $V \in \Omega_d$. By assumption H2, it follows that $\varphi_D(V^+) \in S_{D,p}$.

The forbidden states can remain in $S_{D,f}$ or switch to $S_{D,p}$ since, given any $X \in S_{D,f}$, we have

$$X^+ = F_{b,syn}(X) = \psi(X) \in \Omega = S_{D,p} \cup S_{D,f}.$$

To see that the asynchronous updating strategy also prevents transitions from $S_{D,p}$ to $S_{D,f}$, consider $X \in S_{D,p}$ and any asynchronous transition, $Y = F_{b,asyn}(X)$. If X is an equilibrium point then immediately $Y = X \in S_{D,p}$. Otherwise, since X is of the form (13), it can be written as:

$$X = (\vec{1}_{p_1}, \vec{0}_{d_1-p_1}; \cdots; \vec{1}_{p_M}, \vec{0}_{d_M-p_M}),$$

where $\vec{1}_p$ (resp., $\vec{0}_p$) is a vector of length p with all coordinates equal to 1 (resp., 0). Its synchronous successor is

$$X^+ = (\vec{1}_{p_1^+}, \vec{0}_{d_1-p_1^+}; \cdots; \vec{1}_{p_M^+}, \vec{0}_{d_M-p_M^+}),$$

where $p_i^+ \in \{p_i - 1, p_i, p_i + 1\}$, for all $i = 1, \ldots, M$. Since X is not an equilibrium point, then there exists $k \in \{1, d_M\}$ such that $p_k^+ \neq p_k$. In any asynchronous successor, only one p_i can change at a time. Therefore, there exists exactly one index $1 \leq k \leq M$ such that $p_k^+ = p_k \pm 1$:

$$Y = (\vec{1}_{p_1}, \vec{0}_{d_1-p_1}; \cdots; \vec{1}_{p_k^+}, \vec{0}_{d_1-p_k^+}; \cdots; \vec{1}_{p_M}, \vec{0}_{d_M-p_M}).$$

Therefore, it is clear that $Y \in S_{D,p}$. ∎

2 Multi-level and Boolean state transition tables for *crp*

To write the discrete and Boolean for *crp*, we will divide into the case $U = 0$ and the case $U = 1$. Let $h_{C1}^{0,1}$ and $h_{C2}^{0,1}$ denote the rules for the Boolean variables in the presence or absence of U:

$$\begin{aligned} C_1^+ &= (\overline{U} \wedge h_{C1}^0) \vee (U \wedge h_{C1}^1) \\ C_2^+ &= (\overline{U} \wedge h_{C2}^0) \vee (U \wedge h_{C2}^1) \end{aligned}$$

The grey shaded rows in each Table represent the forbidden states, in $S_{D,f}$. The rules can be written in the form:

$$\begin{aligned} C_1^+ &= (\overline{U} \wedge 1) \vee (U \wedge 1) \equiv 1 \\ C_2^+ &= (\overline{U} \wedge C_1 \wedge \overline{F_1}) \vee (U \wedge (\overline{F_2} \wedge \overline{F_3} \wedge \overline{F_4} \wedge C_1)). \end{aligned}$$

Table 2: Multi-level model for *crp* (C), case $U = 0$.

C	F	C^+	C_1^+	C_2^+
0	0	1	1	0
0	≥ 1	1	1	0
1	0	2	1	1
1	≥ 1	1	1	0
2	0	2	1	1
2	≥ 1	1	1	0

Table 3: Boolean rules for *crp* (C), case $U = 0$.

C_1	C_2	F	C_1^+	C_2^+
0	0	0	1	0
0	0	≥ 1	1	0
0	1	0	1	0
0	1	≥ 1	1	0
1	0	0	1	1
1	0	≥ 1	1	0
1	1	0	1	1
1	1	≥ 1	1	0

Table 4: Multi-level and Boolean rules for *crp*, case $U = 1$.

C	Y	F	C^+	C_1^+	C_2^+
0	0	< 2 ≥ 2	1 1	1 1	0 0
0	1	< 2 ≥ 2	1 1	1 1	0 0
0	2	< 2 ≥ 2	1 1	1 1	0 0
1	0	< 2 ≥ 2	2 1	1 1	1 0
1	1	< 2 ≥ 2	2 1	1 1	1 0
1	2	< 2 ≥ 2	2 1	1 1	1 0
2	0	< 2 ≥ 2	2 1	1 1	1 0
2	1	< 2 ≥ 2	2 1	1 1	1 0
2	2	< 2 ≥ 2	2 1	1 1	1 0

Table 5: Multi-level model for *cya* (Y) (synchronous).

C	Y	U	Y^+	Y_1^+	Y_2^+
0	0	0 1	1 1	1 1	0 0
0	1	0 1	2 2	1 1	1 1
0	2	0 1	2 2	1 1	1 1
1	0	0 1	1 1	1 1	0 0
1	1	0 1	2 2	1 1	1 1
1	2	0 1	2 2	1 1	1 1
2	0	0 1	1 1	1 1	0 0
2	1	0 1	2 2	1 1	1 1
2	2	0 1	2 1	1 1	1 0

Table 6: Boolean rules for *cya*.

C_1	C_2	Y_1	Y_2	U	Y_1^+	Y_2^+
0	0	0	0	0 1	1 1	0 0
0	0	0	1	0 1	1 1	0 0
0	0	1	0	0 1	1 1	1 1
0	0	1	1	0 1	1 1	1 1
0	1	0	0	0 1	1 1	0 0
0	1	0	1	0 1	1 1	0 0
0	1	1	0	0 1	1 1	1 1
0	1	1	1	0 1	1 1	1 1
1	0	0	0	0 1	1 1	0 0
1	0	0	1	0 1	1 1	0 0
1	0	1	0	0 1	1 1	1 1
1	0	1	1	0 1	1 1	1 1
1	1	0	0	0 1	1 1	0 0
1	1	0	1	0 1	1 1	0 0
1	1	1	0	0 1	1 1	1 1
1	1	1	1	0 1	1 1	1 0

Table 7: Multi-level model for *gyrAB* (G) and *topA* (T) (synchronous).

G	T	F	G^+	T^+	G_1^+	G_2^+	T_1^+	T_2^+
0	0	$< 3 \geq 3$	1 0	0 0	1 0	0 0	0 0	0 0
0	1	$< 3 \geq 3$	1 0	0 0	1 0	0 0	0 0	0 0
0	2	$< 3 \geq 3$	1 0	1 1	1 0	0 0	1 1	0 0
1	0	$< 3 \geq 3$	2 0	0 0	1 0	1 0	0 0	0 0
1	1	$< 3 \geq 3$	2 0	0 0	1 0	1 0	0 0	0 0
1	2	$< 3 \geq 3$	2 0	1 1	1 0	1 0	1 1	0 0
2	0	$< 3 \geq 3$	1 1	0 1	1 1	0 0	0 1	0 0
2	1	$< 3 \geq 3$	2 1	0 0	1 1	1 0	0 0	0 0
2	2	$< 3 \geq 3$	2 1	1 1	1 1	1 0	1 1	0 0

3 Multi-level and Boolean state transition tables for *cya*

The two columns under U, Y_1^+ or Y_2^+ correspond to the cases $U = 0$ or $U = 1$. The corresponding Boolean rules can be written:

$$\begin{aligned} Y_1^+ &= 1 \\ Y_2^+ &= (\overline{U} \wedge Y_1) \vee (U \wedge [(Y_1 \wedge (\overline{C_1} \vee \overline{C_2})) \vee ((Y_1 \wedge \overline{Y_2}) \wedge C_1 \wedge C_2)]) \end{aligned}$$

Table 8: Boolean rules for *gyrAB* and *topA*.

G_1	G_2	T_1	T_2	F	G_1^+	G_2^+	T_1^+	T_2^+
0	0	0	0	$< 3 \geq 3$	1 0	0 0	0 0	0 0
0	0	0	1	$< 3 \geq 3$	1 0	0 0	1 1	0 0
0	0	1	0	$< 3 \geq 3$	1 0	0 0	0 0	0 0
0	0	1	1	$< 3 \geq 3$	1 0	0 0	1 1	0 0
0	1	0	0	$< 3 \geq 3$	1 1	0 0	0 1	0 0
0	1	0	1	$< 3 \geq 3$	1 1	0 0	1 1	0 0
0	1	1	0	$< 3 \geq 3$	1 1	0 0	0 0	0 0
0	1	1	1	$< 3 \geq 3$	1 1	0 0	1 1	0 0
1	0	0	0	$< 3 \geq 3$	1 0	1 0	0 0	0 0
1	0	0	1	$< 3 \geq 3$	1 0	1 0	1 1	0 0
1	0	1	0	$< 3 \geq 3$	1 0	1 0	0 0	0 0
1	0	1	1	$< 3 \geq 3$	1 0	1 0	1 1	0 0
1	1	0	0	$< 3 \geq 3$	1 1	0 0	0 1	0 0
1	1	0	1	$< 3 \geq 3$	1 1	1 0	1 1	0 0
1	1	1	0	$< 3 \geq 3$	1 1	1 0	0 0	0 0
1	1	1	1	$< 3 \geq 3$	1 1	1 0	1 1	0 0

4 Multi-level and Boolean state transition tables for *gyrAB* and *topA*

The corresponding Boolean rules can be written:

$$\begin{aligned}
G_1^+ &= [\overline{F_3} \wedge \overline{F_4}] \vee [(F_1 \wedge F_2 \wedge F_3) \vee G_2] \\
G_2^+ &= \overline{F_3} \wedge \overline{F_4} \wedge G_1 \wedge (\overline{G_2} \vee T_1 \vee T_2) \\
T_1^+ &= [\overline{F_3} \wedge \overline{F_4} \wedge T_2] \vee [F_1 \wedge F_2 \wedge F_3 \wedge ((\overline{G_2} \wedge T_2) \vee (G_2 \wedge (T_2 \vee \overline{T_1})))] \\
T_2^+ &= 0.
\end{aligned}$$

5 Multi-level and Boolean state transition tables for *fis*

The rules for *fis* will also be determined separately for $U = 0$ and $U = 1$. Let H_i^0 (resp., H_i^0) denote the rules for the Boolean variable F_i in the absence (resp., presence) of U:

$$\begin{aligned}
F_1 &= (\overline{U} \wedge H_1^0) \vee (U \wedge H_1^1) \\
F_2 &= (\overline{U} \wedge H_2^0) \vee (U \wedge H_2^1) \\
F_3 &= (\overline{U} \wedge H_3^0) \vee (U \wedge H_3^1) \\
F_4 &= (\overline{U} \wedge H_4^0) \vee (U \wedge H_4^1)
\end{aligned}$$

The Boolean rules for *fis*, in the case $U = 0$, can be written:

Table 9: Multi-level model for *fis*, case $U = 0$.

G	T	F	F^+
0	0	0 1 2 3 4	1 1 1 2 3
0	1	0 1 2 3 4	1 1 1 2 3
0	2	0 1 2 3 4	1 1 1 2 3
1	0	0 1 2 3 4	1 2 3 4 3
1	1	0 1 2 3 4	1 2 3 4 3
1	2	0 1 2 3 4	1 1 1 2 3
2	0	0 1 2 3 4	1 2 3 4 3
2	1	0 1 2 3 4	1 2 3 4 3
2	2	0 1 2 3 4	1 1 1 2 3

Table 10: Boolean rules for *fis*, case $U = 0$.

G_1	G_2	T_1	T_2	F	F_1^+	F_2^+	F_3^+	F_4^+
0	0	0	0	0 1 2 3 4	1 1 1 1 1	0 0 0 1 1	0 0 0 0 1	0 0 0 0 0
0	0	0	1	0 1 2 3 4	1 1 1 1 1	0 0 0 1 1	0 0 0 0 1	0 0 0 0 0
0	0	1	0	0 1 2 3 4	1 1 1 1 1	0 0 0 1 1	0 0 0 0 1	0 0 0 0 0
0	0	1	1	0 1 2 3 4	1 1 1 1 1	0 0 0 1 1	0 0 0 0 1	0 0 0 0 0
0	1	0	0	0 1 2 3 4	1 1 1 1 1	0 0 0 1 1	0 0 0 0 1	0 0 0 0 0
0	1	0	1	0 1 2 3 4	1 1 1 1 1	0 0 0 1 1	0 0 0 0 1	0 0 0 0 0
0	1	1	0	0 1 2 3 4	1 1 1 1 1	0 0 0 1 1	0 0 0 0 1	0 0 0 0 0
0	1	1	1	0 1 2 3 4	1 1 1 1 1	0 0 0 1 1	0 0 0 0 1	0 0 0 0 0
1	0	0	0	0 1 2 3 4	1 1 1 1 1	0 1 1 1 1	0 0 1 1 1	0 0 0 1 0
1	0	0	1	0 1 2 3 4	1 1 1 1 1	0 0 0 1 1	0 0 0 0 1	0 0 0 0 0
1	0	1	0	0 1 2 3 4	1 1 1 1 1	0 1 1 1 1	0 0 1 1 1	0 0 0 1 0
1	0	1	1	0 1 2 3 4	1 1 1 1 1	0 0 0 1 1	0 0 0 0 1	0 0 0 0 0
1	1	0	0	0 1 2 3 4	1 1 1 1 1	0 1 1 1 1	0 0 1 1 1	0 0 0 1 0
1	1	0	1	0 1 2 3 4	1 1 1 1 1	0 0 0 1 1	0 0 0 0 1	0 0 0 0 0
1	1	1	0	0 1 2 3 4	1 1 1 1 1	0 1 1 1 1	0 0 1 1 1	0 0 0 1 0
1	1	1	1	0 1 2 3 4	1 1 1 1 1	0 0 0 1 1	0 0 0 0 1	0 0 0 0 0

Table 11: Multi-level model for *fis*, case $U = 1$ and $C = 0$ or $Y = 0$.

C	Y	G	T	F	F^+
		0	0	0 1 2 3 4	1 1 1 2 3
		0	1	0 1 2 3 4	1 1 1 2 3
		0	2	0 1 2 3 4	1 1 1 2 3
0	*	1	0	0 1 2 3 4	1 2 3 4 3
		1	1	0 1 2 3 4	1 2 3 4 3
*	0	1	2	0 1 2 3 4	1 1 1 2 3
		2	0	0 1 2 3 4	1 2 3 4 3
		2	1	0 1 2 3 4	1 2 3 4 3
		2	2	0 1 2 3 4	1 1 1 2 3
1,2	1,2	*	*	0 1 2 3 4	0 0 1 2 3

Table 12: Boolean rules for *fis*, case $U = 1$, and $C, Y \in \{1, 2\}$.

C_1	C_2	Y_1	Y_2	F	F_1^+	F_2^+	F_3^+	F_4^+
0	1	0	1	0 1 2 3 4	0 0 1 1 1	0 0 0 1 1	0 0 0 0 1	0 0 0 0 0
0	1	1	0	0 1 2 3 4	0 0 1 1 1	0 0 0 1 1	0 0 0 0 1	0 0 0 0 0
0	1	1	1	0 1 2 3 4	0 0 1 1 1	0 0 0 1 1	0 0 0 0 1	0 0 0 0 0
1	0	0	1	0 1 2 3 4	0 0 1 1 1	0 0 0 1 1	0 0 0 0 1	0 0 0 0 0
1	0	1	0	0 1 2 3 4	0 0 1 1 1	0 0 0 1 1	0 0 0 0 1	0 0 0 0 0
1	0	1	1	0 1 2 3 4	0 0 1 1 1	0 0 0 1 1	0 0 0 0 1	0 0 0 0 0
1	1	0	1	0 1 2 3 4	0 0 1 1 1	0 0 0 1 1	0 0 0 0 1	0 0 0 0 0
1	1	1	0	0 1 2 3 4	0 0 1 1 1	0 0 0 1 1	0 0 0 0 1	0 0 0 0 0
1	1	1	1	0 1 2 3 4	0 0 1 1 1	0 0 0 1 1	0 0 0 0 1	0 0 0 0 0

$$
\begin{aligned}
H_1^0 &= 1 \\
H_2^0 &= (F_1 \wedge G_1 \wedge \overline{T_2}) \vee (F_1 \wedge F_2 \wedge F_3) \\
H_3^0 &= (F_1 \wedge F_2 \wedge G_1 \wedge \overline{T_2}) \vee (F_1 \wedge F_2 \wedge F_3 \wedge F_4) \\
H_4^0 &= (F_1 \wedge F_2 \wedge F_3 \wedge \overline{F_4} \wedge G_1 \wedge \overline{T_2}).
\end{aligned}
$$

The Boolean rules for *fis*, in the case $U = 1$, can be written:

$$
\begin{aligned}
H_1^1 &= [((\overline{C_1} \wedge \overline{C_2}) \vee (\overline{Y_1} \wedge \overline{Y_2})) \wedge H_1^0] \vee [(C_1 \vee C_2 \vee Y_1 \vee Y_2) \wedge F_1 \wedge F_2] \\
H_2^1 &= [((\overline{C_1} \wedge \overline{C_2}) \vee (\overline{Y_1} \wedge \overline{Y_2})) \wedge H_2^0] \vee [(C_1 \vee C_2 \vee Y_1 \vee Y_2) \wedge F_1 \wedge F_2 \wedge F_3] \\
H_3^1 &= [((\overline{C_1} \wedge \overline{C_2}) \vee (\overline{Y_1} \wedge \overline{Y_2})) \wedge H_3^0] \vee [(C_1 \vee C_2 \vee Y_1 \vee Y_2) \wedge F_1 \wedge F_2 \wedge F_3 \wedge F_4] \\
H_4^1 &= [((\overline{C_1} \wedge \overline{C_2}) \vee (\overline{Y_1} \wedge \overline{Y_2})) \wedge H_4^0].
\end{aligned}
$$

Centre de recherche INRIA Sophia Antipolis – Méditerranée
2004, route des Lucioles - BP 93 - 06902 Sophia Antipolis Cedex (France)

Centre de recherche INRIA Bordeaux – Sud Ouest : Domaine Universitaire - 351, cours de la Libération - 33405 Talence Cedex
Centre de recherche INRIA Grenoble – Rhône-Alpes : 655, avenue de l'Europe - 38334 Montbonnot Saint-Ismier
Centre de recherche INRIA Lille – Nord Europe : Parc Scientifique de la Haute Borne - 40, avenue Halley - 59650 Villeneuve d'Ascq
Centre de recherche INRIA Nancy – Grand Est : LORIA, Technopôle de Nancy-Brabois - Campus scientifique
615, rue du Jardin Botanique - BP 101 - 54602 Villers-lès-Nancy Cedex
Centre de recherche INRIA Paris – Rocquencourt : Domaine de Voluceau - Rocquencourt - BP 105 - 78153 Le Chesnay Cedex
Centre de recherche INRIA Rennes – Bretagne Atlantique : IRISA, Campus universitaire de Beaulieu - 35042 Rennes Cedex
Centre de recherche INRIA Saclay – Île-de-France : Parc Orsay Université - ZAC des Vignes : 4, rue Jacques Monod - 91893 Orsay Cedex

Éditeur
INRIA - Domaine de Voluceau - Rocquencourt, BP 105 - 78153 Le Chesnay Cedex (France)
http://www.inria.fr
ISSN 0249-6399